Journal of Non-Crystalline Solids 458 (2017) 65–68

Contents lists available at ScienceDirect

Journal of Non-Crystalline Solids

journal homepage: www.elsevier.com/locate/jnoncrysol

Optical and structural properties of neodymium-doped KPO_3-MoO_3 glasses

Gustavo Galleani [a], Silvia H. Santagneli [a,*], Sidney J.L. Ribeiro [a], Younes Messaddeq [a], Lauro J.Q. Maia [b], Luiz A.O. Nunes [c]

[a] Institute of Chemistry, São Paulo State University/UNESP, CP355 Araraquara-SP, 14801-970, Brazil
[b] Institute of Physics, Federal University of Goiás/UFG, Goiânia, GO, Brazil
[c] Institute of Physics of São Carlos, São Paulo University/USP, São Carlos, SP, Brazil

ARTICLE INFO

Article history:
Received 12 June 2016
Received in revised form 29 November 2016
Accepted 2 December 2016
Available online 18 December 2016

Keywords:
Phosphate glasses
Nd^{3+} ions
Optical properties
Lifetime

ABSTRACT

Glasses of composition (mol%) 75KPO_3-(25-x)MoO_3-xNd^{3+}, with $0 \le x \le 1.0$, have been prepared and characterized. Thermal and structural properties of the glasses were studied by Differential Scanning Calorimetry (DSC) and Raman scattering spectroscopy. The thermal stability against crystallization on heating was evaluated. Absorption spectra in the visible and infrared regions were collected and analysed, and photoluminescence excitation and emission spectra were obtained under 804 nm diode laser excitations. Using the Judd-Ofelt formalism, the Ω_2, Ω_4, and Ω_6 parameters and the radiative lifetime (τ_r) were calculated for the $^4F_{3/2}$ excited state. A fluorescence quantum efficiency for this level ($QE = \tau_f / \tau_r$) of 58% was determined for glass with x = 0.6.

1. Introduction

The utilization of rare earth (RE) ions based materials has received considerable attention because of their potential applications including three-dimensional displays [1], laser and optical amplifiers [2], solar cells [3,4], bio-technologies [5,6,7].

The application of Nd^{3+} for high power laser design has been known for the past several decades and a lot of work has been carried out on the spectroscopic and lasing characteristics of Nd^{3+} ion in both crystalline and amorphous matrices [8]. The tailoring of fluorescence and up-conversion properties of Nd^{3+} ions to a considerable extent could be attained by suitably selecting the host matrix [9,10].

The selection of the host matrix is an important factor to obtain highly efficient luminescence since the widths and relative intensities of these lines are dependent on the host matrix. These features can be used to tune the emission of the material depending on their practical applications [11,12]. In this sense, glassy materials have been suited to several optical applications. They are easy to fabricate into waveguide form and in bulk, in comparison to crystalline materials [13,14]. Different glass family hosts, including borates, phosphates, fluorides, germanates, vanadates and tellurites have been studied extensively for this purpose [3,8,9,15,16]. Among these families, borate and phosphate glasses are well known to incorporate high concentrations of rare-earth ions [17].

Campbell and Suratwala [18] published a review on neodymium-doped phosphate glasses used for high energy (10^3–10^6 J) and high-peak-power (10^{12}–10^{15} W) laser applications such as fusion energy research. The most common base glasses are meta-phosphates (O/P ~ 3) with the approximate composition: 60P_2O_5-10Al_2O_3-30M_2O/MO; K/Ba or K/Mg are typical modifiers.

Recently, studies have been presented in phosphate - molybdenum oxide glasses and their optical properties [19,20]. The use of this glassy family have been one challenge due to formation of reduced species Mo^{5+} and Mo^{4+} species. Poirier et al. [19] observed that an increase of the MoO_3 concentration promotes a strong absorption in the visible and near infrared attributed to Mo atoms reduction during glass synthesis. Octahedral coordination is proposed for Mo atoms and a large proportion of reduced species Mo^{5+} and Mo^{4+} of electronic configurations d^1 and d^2 is present. Optical applications for Molybdenum oxide containing glasses have been limited by the poor transparency in the visible and near infrared due to the absorption of reduced Mo species, resulting in dark green, brown and black glasses [19,21]. Using phosphate glasses could be useful in the control of Mo reduction process that occurs during the synthesis or in compositions where the reduction is not favored [22]

In this context, this work presents results for the optical and thermal properties of 75KPO_3-(25-x)MoO_3-xNd^{3+} glass system, with x varying

* Corresponding author.
E-mail address: santagneli@iq.unesp.br (S.H. Santagneli).

http://dx.doi.org/10.1016/j.jnoncrysol.2016.12.002

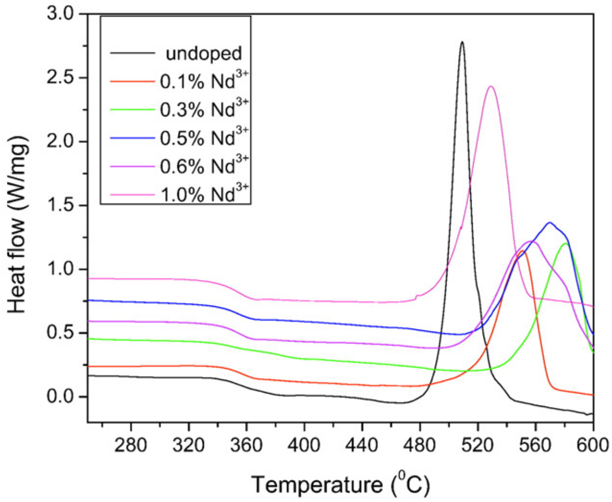

Fig. 1. Differential scanning calorimetry curves of the 75KPO_3-(25-x)MoO_3-x$NdO_{1.5}$ glass compositions.

from 0 to 1.0 in mol%. The experimental results from the fluorescence study are treated within the Judd-Ofelt theoretical approach [23–25].

2. Experimental procedure

2.1. Glass synthesis

The precursor KPO_3 was prepared from decomposition of KH_2PO_4 (Aldrich, 99%) at 330 °C during 24 h and 1000 °C during 24 h in an electric furnace. Vitreous samples in the binary system 75(KPO_3)-(25-x)MoO_3-x$NdO_{1.5}$ with x = 0.0 to 1.0 mol% were prepared by the conventional melt-quenching method using molybdenum oxide (Sigma, 99.5%), potassium polyphosphate prepared previously and Nd_2O_3 (99.5%). The powdered starting materials were mixed and melted in a platinum crucible at a temperature of 750 °C. The resulting liquid was kept at this temperature for 60 min to ensure fine homogenization. Finally, the melts were fast cooled in a brass mold set at 10 °C below the glass transition temperature. All samples presented chemically stable against moisture and a yellow colour suggesting the absence of molybdenum in low valence states. Nd^{3+} doped glasses were polished for the optical characterizations.

2.2. Structural and thermal characterizations

The glass amorphous state was checked by X-ray powder diffraction (X-ray diffractograms not shown here). DSC measurements were conducted with a TA Instruments 2910 calorimeter using a heating rate of 10 °C min^{-1}. Raman scattering spectra measurements were obtained with a LabRam HR instrument of Horiba-Jobin Yvon operating with a He-Ne laser at 632 nm.

2.3. Spectroscopy studies

The visible-infrared absorption spectra were obtained using a Varian Cary 500 spectrophotometer. The measurements were performed on the polished glass discs of 2 mm in thickness and with spectral resolution of 0.5 nm. The refractive index of the glass was measured for transverse electric with an *m*-line apparatus (Metricon Model 2010) based on the prism coupling technique. The resolution in the determination of the angles synchronous to the propagation modes was 0.0075°. Density measurement was performed in a He pycnometer, using a Micromeritics AccuPyc 1330. Experimental oscillator strengths (f_{exp}) of the transitions were evaluated experimentally from integrated absorbance for each band. Afterwards the values obtained were used in order to obtained the so-called Judd-Ofelt intensity parameters (Ω_λ $\lambda = 2, 4, 6$) [25].

Photoluminescence spectroscopy was studied by excitation and emission spectra obtained in a Fluorolog FL-322 spectrofluorimeter of Horiba-Jobin Yvon, equipped with a Hamamatsu photomultiplier for the 250–850 nm range, and an InGaAs photodetector for the 850–1700 nm range. A diode laser diode operating at 804 nm was utilized also as excitation source, by focusing the laser beam on the sample surface through a 100 mm focal length lens, with spectral resolution of 1 nm. All measurements have been performed at room temperature. The luminescence lifetime measurements of the $^4F_{3/2}$ level were obtained using 808 nm wavelength radiation generated by an optical parametric oscillator (OPO) pumped by a 5 ns pulsed Nd:YAG laser (355 nm, 10 Hz).

3. Results and discussion

Fig. 1 shows DSC curves obtained for the all glass samples. The characteristic temperatures (Glass transition (T_g), crystallization onset (T_x) and crystallization maximum (T_p) temperatures) are summarized in Table 1. The value of T_g, T_x and T_p for undoped glass sample could be observed at $T_g = 344$ °C, $T_x = 484$ °C and $T_p = 509$ °C. Thermal stability of the glass was evaluated with the $K_2 = T_x - T_g$ parameter proposed by Hruby [26,27]. The value so obtained of 140 °C, is in agreement with literature [27,29]. Saad and Poulain proposed another parameter the $K_{SP} = (T_x - T_g)(T_p - T_x)/T_g$ which is equal to 10.17 °C. All these values are considered high, which means the glass matrix displays high thermal stability against crystallization on heating [28]. The replacement of molybdenum oxide by Neodymium oxide leads to a small decrease of glass transition temperature (T_g), as can be observed in Fig. 1. The crystallization maximum temperature (T_p) increases from 0 to 0.3 mol% of Nd^{3+} and decreases between 0.3 and 1.0 mol%.

Raman spectra obtained for all glasses are shown in Fig. 2. Phosphate – molybdenum oxide glasses have been studied before by some of us. Additionally to typical phosphate modes glasses P—O—Mo stretching vibrations could be identified [27,29]. The addition of Nd^{3+} to the glassy matrix did not structurally change the network.

The optical absorption spectra from 390 to 1000 nm of the glasses samples with different Nd^{3+} concentrations are presented in Fig. 3. Six main absorption bands are observed at 512, 525, 583,

Table 1
Physical properties of 75KPO_3-(25-x)MoO_3-x$NdO_{1.5}$ glasses.

Glass *x* (mol)	Temperatures (°C)			Thermal stability parameter (°C)	
	Tg (±2)	Tx (±2)	Tp (±1)	K_2 = (Tx − Tg)	$K_{SP} = (T_x - T_g)(T_p - T_x)/T_g$
0	344	484	509	140	10.17
0.1	342	478	551	136	29.03
0.3	340	542	578	202	19.45
0.5	339	521	571	182	26.84
0.6	337	502	556	165	26.44
1.0	335	477	530	142	22.45

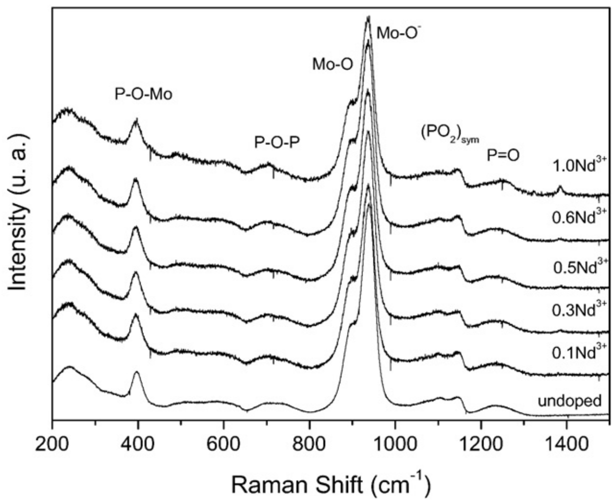

Fig. 2. Raman spectra of the 75KPO_3-(25-x)MoO_3-x$NdO_{1.5}$ glass compositions.

747, 803 and 874 nm for all samples, corresponding to the absorption from $^4I_{9/2}$ fundamental level to the excited electronic states of Nd^{3+} ions, $^2G_{9/2}+{}^4G_{11/2}+{}^2K_{15/2}+{}^2D_{3/2}$, $^2G_{7/2}+{}^4G_{9/2}+{}^2K_{13/2}$, $^4F_{7/2}+{}^4S_{3/2}$, $^4G_{5/2}+{}^2G_{7/2}$, $^4F_{3/2}$, $^4F_{5/2}+{}^2H_{9/2}$ [30]. As mentioned in the Introduction glasses containing molybdenum oxide in general display colors due to Mo reduced species. Interestingly enough, samples studied here presented high transparency (higher than 80%) between 430 and 1000 nm, suggesting no absorbing species. The increasing absorbance in the UV relates to the glass host bandgap that could be identified here at 2.96 eV.

Table 2 shows the values for experimental oscillator strengths f_{exp} obtained for all glass compositions doped with Nd^{3+}, using for calculated the density 2.768 g·cm^{-3} and refractive index 1.6362 obtained at 532 nm values. The intensity parameters and the calculated oscillator strengths obtained by using standard methods are also presented [25].

The obtained values of the phenomenological intensity parameters Ω_2, Ω_4 and Ω_6 are shown in Table 3. The calculated values are in the range of observed intensity parameters for Nd^{3+} in different phosphate glasses [31]. These values obtained were used to calculate the radiative transition probabilities ($A_{j\rightarrow j'}$) for the excited $^4F_{3/2}$ to ^4I_j, manifold ($^4I_{9/2}$, $^4I_{11/2}$, $^4I_{13/2}$ and $^4I_{15/2}$) for Nd^{3+} and the branching ratios ($\beta_{J\rightarrow J'}$). The

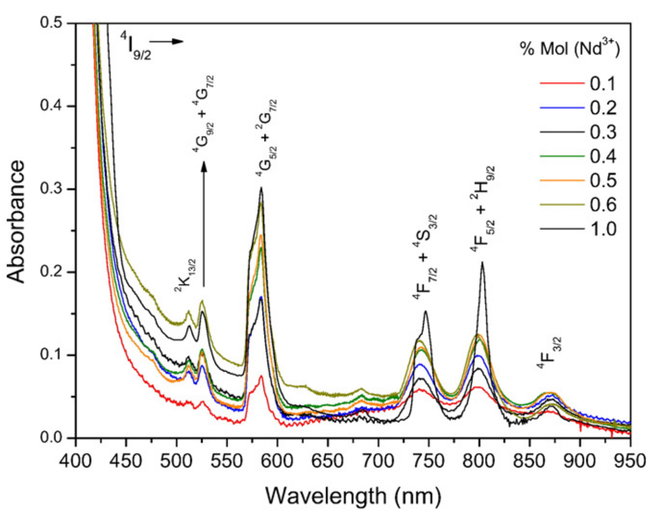

Fig. 3. Optical absorption spectrum of the glass doped with 0.6 mol% Nd^{3+}. Inset shows the intensity for the transition $^4G_{5/2}+{}^2G_{7/2}$ as a function Nd^{3+} concentration.

Table 2
Experimental and calculated oscillator strengths (f × 10^{-6}) values of absorption transitions of the glasses contained different concentration of the Nd^{3+} ions doped composition.

Transitions	Energy (cm^{-1})	0.5% Nd^{3+}		0.6% Nd^{3+}		1.0% Nd^{3+}	
		f_{exp}	f_{cal}	f_{exp}	f_{cal}	f_{exp}	f_{cal}
$^4F_{3/2}$	11,455	2.52	2.05	0.85	0.70	0.60	0.71
$^4F_{5/2}+{}^2H_{9/2}$	12,453	4.45	4.80	3.30	2.79	2.61	2.40
$^4F_{7/2}+{}^4S_{3/2}$	13,387	4.35	4.10	2.86	3.10	2.39	2.51
$^4G_{5/2}+{}^2G_{7/2}$	17,123	16.0	16.0	12.0	11.9	7.66	7.65
$^4G_{7/2}+{}^4G_{9/2}+{}^2K_{13/2}$	19,029	3.38	4.48	1.78	2.31	1.85	1.93
rms		0.95 × 10^{-6}		0.64 × 10^{-6}		0.12 × 10^{-6}	

radiative rates for all four transitions and the branching ratios are shown in Table 4. The branching ratio values are known to be related to the Ω_4/Ω_6 ratio value (see Table 3). For most glasses $\Omega_4 < \Omega_6$ and the largest transition probability is to the $^4I_{11/2}$ [30], in agreement with our molybdenum phosphate glass contained high concentration of the neodymium ions. The obtained total radiative rates are 2486.37, 2639.15 and 1725.49 s^{-1} of the $^4F_{3/2}$ metastable state for the samples with 0.5, 0.6 and 1.0 mol% Nd^{3+}, respectively. The radiative lifetime, τ_r, for the $^4F_{3/2}$ excited state is calculated by equation

$$\tau_r=\frac{1}{\sum A(J\rightarrow J')}$$

and obtained are shown in Table 4, the results are nearly the same for other phosphate glasses in literature [32].

Photoluminescence spectra obtained for excitation at 804 nm and lifetime decay curves are shown in Figs.s 4 and 5, respectively. A mean decay time of around 220 μs was obtained from the integrated decay curves for all samples. The radiative lifetime (τ_r) of the $^4F_{3/2}$ state determined by the Judd-Ofelt analysis was found to be 379 μs, resulting in the fluorescence quantum efficiency ($QE = \tau_f / \tau_r$) of 58%, similar to fluorophosphates glasses [32] and phosphate glasses [33] found in the literature.

4. Conclusion

New phosphate-molybdenum oxide glasses were prepared. From DSC curves some thermal parameters as T_g, T_x and T_p were measured and used to determined thermal stability parameters from equations proposed by Hruby (K_2) and Saad and Poulain (K_{SP}) being 140 °C and 10.17 °C, respectively, showing that the glass matrix possess a high thermal stability against crystallization on heating. The addition of MoO_3 to KPO_3 glass produces P—O—Mo connectivities leading to a special stability of the glasses. The addition of neodymium to the glassy matrix did not structurally change the network. Nd^{3+} spectroscopic characteristics were analysed. Under excitation at 804 nm with a diode laser IR emission was obtained. Judd-Ofelt intensity parameters were obtained for the sample with 0.6% Nd^{3+} with values $\Omega_2 = 3.2\times10^{-20}$ cm^{-2}, $\Omega_4 = 1.6\times10^{-20}$ cm^{-2} and $\Omega_6 = 2.6\times10^{-20}$ cm^{-2}. The calculated radiative lifetime (τ_r) for the $^4F_{3/2}$ excited state is 379 μs, and a measured room temperature lifetime (τ_f) were found to be ~220 μs, with no considerable variation with the measured lifetime with the concentration, leading to a fluorescence quantum efficiency ($QE = \tau_f / \tau_r$) of 58%, being similar to other phosphate glasses in literature. On the other

Table 3
Calculated Judd-Ofelt intensity parameters $\Omega_{2,4,6}$ (10^{-20} cm^2), spectroscopic quality factor (Ω_4/Ω_6) for glass samples doped with Nd^{3+} ions.

Nd^{3+} (x mol%)	Ω_2	Ω_4	Ω_6	Ω_4/Ω_6
0.5	2.8 ± 0.5	4.2 ± 0.5	2.4 ± 0.5	1.75
0.6	2.9 ± 0.4	1.3 ± 0.4	2.1 ± 0.4	0.62
1.0	2.3 ± 0.9	1.4 ± 0.9	2.0 ± 0.9	0.70

Table 4
Radiative transition probabilities ($A_{j\rightarrow j'}$) and the branching ratios ($\beta_{j\rightarrow j'}$) for the excited $^4F_{3/2}$ to ^4I_j manifold ($^4I_{9/2}$, $^4I_{11/2}$, $^4I_{13/2}$ and $^4I_{15/2}$) of glass composition contained 0.5, 0.6 and 1.0% Nd^{3+}.

Transition	Wavenumber (cm^{-1})	0.5% Nd^{3+}		0.6% Nd^{3+}		1.0% Nd^{3+}	
		$A_{j\rightarrow j'}$ (s^{-1})	$\beta_{j\rightarrow j'}$	$A_{j\rightarrow j'}$ (s^{-1})	$\beta_{j\rightarrow j'}$	$A_{j\rightarrow j'}$ (s^{-1})	$\beta_{j\rightarrow j'}$
$^4F_{3/2} \rightarrow {}^4I_{9/2}$	11,415	1020	0.41	975.78	0.37	614.25	0.36
$^4F_{3/2} \rightarrow {}^4I_{11/2}$	9488	1298	0.52	1332.05	0.51	891.61	0.52
$^4F_{3/2} \rightarrow {}^4I_{13/2}$	7541	159.92	0.06	318.34	0.12	211.14	0.12
$^4F_{3/2} \rightarrow {}^4I_{15/2}$	5556	8.447	0.003	12.98	0.05	8.49	0.005
	Nd^{3+} (mol%)	0.5		0.6		1.0	
	$A_t = \sum A(s^{-1})$	2486.37		2639.15		1725.49	
	τ_r (μs)	402.19		378.9		579.5	
	$QE = \tau_f / \tau_r$	0.55		0.58		0.38	

hand, our doped samples possess only visible absorption from Nd^{3+} ions, and absorption from Mo ions with low valences were not detected. Finally, we obtained glassy matrix with high transparency in the visible and near infrared regions.

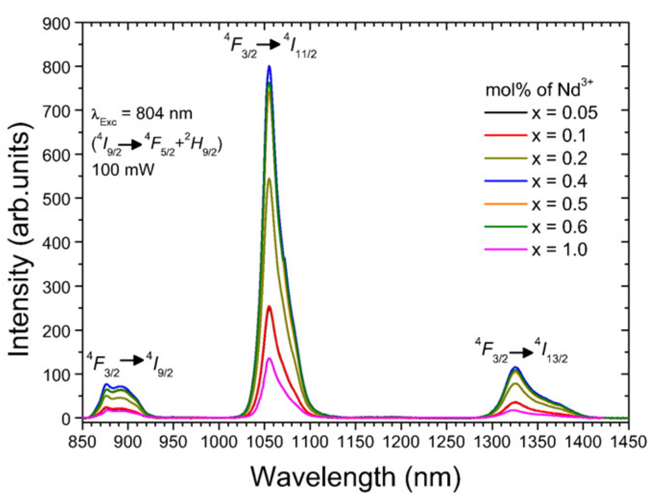

Fig. 4. Near infrared emission spectra of the glasses under 804 nm excitation using a diode laser.

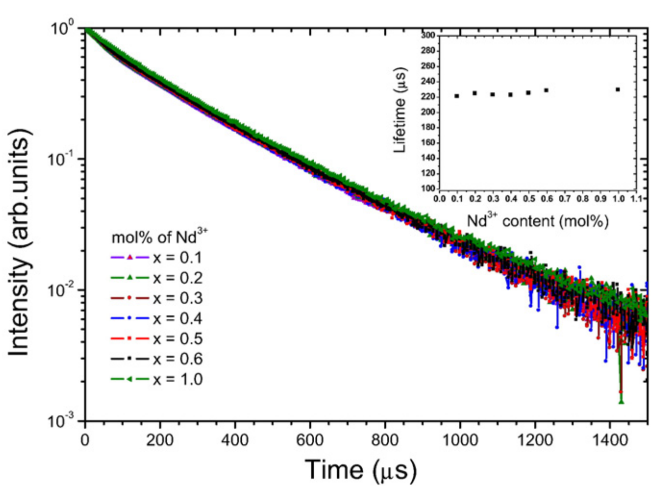

Fig. 5. The fluorescence lifetime decay curves for the emission at 1054 nm.

Acknowledgments

This work was funded by the Brazilian agencies FAPESP (Process n° 08/53680-0), FAPEG, CAPES and CNPq.

References

[1] J. Mendez-Ramos, V.K. Tikhomirov, V.D. Rodriguez, D. Furniss, J. Alloys Compd. 440 (2007) 328–332.
[2] J.H. Zhang, H.Z. Tao, Y. Chang, X.J. Zhao, J. Rare Earth 25 (2007) 100–105.
[3] T. Suzuki, H. Kawai, H. Nasu, S. Mizuno, H. Ito, K. Hasegawa, Y. Ohishi, J. Opt. Soc. Am B 28-8 (2011) 2001–2006.
[4] B.S. Richards, A. Shalav, IEEE Trans. Electron Devices 54 (2007) 2679–2684.
[5] E. Downing, L. Hesselink, J. Ralston, R. Macfarlane, Science 273 (1996) 1185.
[6] A. Rapaport, J. Milliez, M. Bass, A. Cassanho, H. Jenssen, J. Disp. Technol. 2 (2006) 68.
[7] A. Conde-Gallardo, M. Garcia-Rocha, I. Hernandez-Calderon, R. Palomino-Merino, Appl. Phys. Lett. 78 (2001) 3436.
[8] C. Daqin, W. Yuansheng, Y. Yunlong, L. Feng, H. Ping, J. Rare Earths 26 (2008) 428.
[9] C.Y. Chen, W.A. Sibley, D.C. Yeh, C.A. Hunt, J. Lumin. 43 (1989) 185.
[10] R.M. Macfarlane, F. Tong, A.J. Silversmith, W. Lenth, Appl. Phys. Lett. 52 (1988) 1300.
[11] F. Liu, E. Ma, D. Chen, Y. Yu, Y. Wang, J. Phys. Chem. B 110 (2006) 20843.
[12] A. Quach, V. Escax, L. Nicole, P. Goldner, O. Guillot-Noel, P. Aschehoug, P. Hesemann, J. Moreau, D. Gourier, C. Sanchez, J. Mater. Chem. 17 (2007) 2552.
[13] S. Tanabe, K. Tamai, K. Hirao, N. Soga, Phys. Rev. B 53 (1996) 8358.
[14] H. Lin, S. Jiang, J. Wu, F. Song, N. Peyghambarian, E.Y.B. Pun, J. Phys. D. Appl. Phys. 36 (2003) 812.
[15] J.S. Kumar, A.M. Babu, T. Sasikala, L.R. Moorthy, Chem. Phys. Lett. 484 (2010) 207.
[16] M. Yamane, Y. Asahara, Glasses for Photonics, Cambridge University Press, 2000.
[17] E. Lallier, Appl. Opt. 31 (1992) 5276.
[18] J.H. Campbell, T.I. Suratwala, J. Non-Cryst. Solids 263–264 (2000) 318.
[19] G. Poirier, F.C. Cassanjes, Mater. Chem. Phys. 120 (2010) 501.
[20] I. Rosslerova, L. Koudelka, Z. Cernosek, P. Mosner, L. Benes, J. Mater. Sci. 46 (2011) 6751.
[21] B. Sreedhar, M. Sairam, D.K. Chattopadhyay, K. Kojima, Mater. Chem. Phys. 92 (2005) 492.
[22] G. Poirier, F.S. Ottoboni, F.C. Cassanjes, A. Remonte, Y. Messaddeq, S.J.L. Ribeiro, J. Phys. Chem. B 112–115 (2008) 4481–4487.
[23] B.R. Judd, Phys. Rev. 127 (1962) 750.
[24] G.S. Ofelt, J. Chem. Phys. 37 (1962) 511.
[25] L.D. Carlos, R.A.S. Ferreira, V.Z. Bermudez, S.J.L. Ribeiro, Adv. Mater. 21 (2009) 509–534.
[26] S.H. Santagneli, C.C. de Araujo, W. Strojek, H. Eckert, G. Poirier, S.J.L. Ribeiro, Y. Messaddeq, J. Phys. Chem. B 111 (2007) 10109.
[27] L. Koudelka, I. Rosslerová, J. Holubová, P. Mosner, L. Montagne, B. Revel, J. Non-Cryst. Solids 357 (2011) 2816.
[28] A.J. Barbosa, L.J.Q. Maia, A.M. Nascimento, R.R. Gonçalves, G. Poirier, Y. Messaddeq, S.J.L. Ribeiro, J. Non-Cryst. Solids 354 (2008) 4743.
[29] S.H. Santagneli, J. Ren, M.T. Rinke, S.J.L. Ribeiro, Y. Messaddeq, H. Eckert, J. Non-Cryst. Solids 358–6 (2012) 985–992.
[30] M.C. Silva, A.S.S. de Camargo, L.A.O. Nunes, R.A. Silva, A. Marletta, J. Non-Cryst. Solids 354 (2008) 5496.
[31] M.J. Weber, D.C. Ziegler, C.A. Angell, J. Appl. Phys. 53 (1982) 4344.
[32] J. Dong, M. Bass, C. Walters, J. Opt. Soc. Am. B 21 (2004) 454.
[33] H. Ebendorff-Heidepriem, D. Ehrt, M. Bertinelli, A. Speghini, J. Non-Cryst. Solids 240 (1998) 66.